

MODELING OF MICROPOROSITY EVOLUTION DURING SOLIDIFICATION PROCESSES

J. Huang and J.G. Conley

Department of Mechanical Engineering
Northwestern University
Evanston, IL 60208

INTRODUCTION

The occurrence of porosity during alloy solidification is a significant factor in evaluating the quality of metal castings. In general, porosity forms when there is solidification shrinkage, failure of interdendritic feeding or exsolution of dissolved gas from the melt. The existence of porosity in castings is known to negatively effect mechanical properties, such as tensile strength, and fatigue life [1-4]. Foundry process computer simulations that help determine the location, size, shape and extent of porosity can be used by the casting designer to evaluate the probability of detecting porosity by NDE techniques.

Porosity is usually observed in the form of macroscopic holes (~1 to 10 mm) in localized regions or as microporosity (~1 to 500 μm) distributed more or less homogeneously throughout the casting [5]. Macroporosity is usually in the form of massive shrinkage cavities which form because of failure to compensate for solidification shrinkage (~ 8% change in density for A356). It is typically observed at the region of the casting last to solidify. Microporosity, on the other hand is results from either failure of interdendritic feeding or exsolution of dissolved gas in the molten metal. Inclusions also play an important role in microporosity formation. They serve as nucleation sites for the dissolved gas and thus facilitate gas pore formation. For aluminum and magnesium alloys, hydrogen is the only gas that dissolves to a significant extent in the melt [6]. It is a constant source of difficulty for the foundry because it dissolves upon reaction of molten metal with atmospheric humidity and moisture.

There have been a substantial number of investigations into the formation and growth of porosity in aluminum casting alloys. One body of work establishes criteria functions which combine thermal parameters such as thermal gradient, G , cooling rate, R , and cooling time, t_s , to derive an expression for the limiting thermal conditions for feeding of liquid metal to the last regions of the casting to solidify [7-11]. Criteria functions are attractive because of their simplicity and ease of incorporation into existing casting simulation software. However, there is typically no accounting for the effect of hydrogen.

Another body of work attempts to numerically model the formation of microporosity based on first principles [12-15]. Despite the promise of such efforts, these models have

not been widely adopted [8]. It is not easy to incorporate micro-mechanism models to the existing commercial macroscopic heat transfer based casting simulation codes. Additionally, these models do not accurately represent the physical models of pore evolution accurately, i.e. microshrinkage pores can not be accounted for in these models and it is assumed that there is a maximum of one gas pore formed in each computational element.

Casting process and solidification simulations have also been used in an attempt to model the grain structure of the casting. However, as in the case of porosity prediction, the scale used in these grain structure prediction models are too big to capture the micro scale defects. Many of the defects or grain structure are in the scales much smaller than that of the heat transfer problems solved in the models. For that reason, the mathematical models can not provide direct view of the microstructure, such as the evolution of grain and pore morphologies. Realizing the limitation of these mathematical models, a different approach to predict grain structure based upon probabilistic concept was first developed by Spittle and Brown [16] and followed by other researchers [17-20].

In this paper, we present an innovative approach to predict microporosity evolution during solidification processes. The proposed two dimensional model integrates the mathematical model of porosity prediction with probabilistic model of grain nucleation and growth. It is necessary to couple these two models together because the size and location of pores are closely related to dendrite growth and grain structure formation of the solidifying casting. By doing so, not only can the model predict microporosity in terms of the amount of voids, but also the possible size and location of these voids.

MODEL FORMULATION

The mathematical model to predict microporosity evolution during solidification was first proposed by Kubo and Pehlke in 1984 [12]. The governing equations for microporosity evolution in our model follow the work of Kubo and Pehlke closely. However, as will be shown later, by combining the mathematical model with probabilistic microstructure method, our model is able to predict the location, size and volume fraction of porosity.

To mathematically model the formation of microporosity, both macroscopic and microscopic aspects of solidification need to be addressed. Macroscopic models are used to predict the flow pattern and temperature distribution in the mold cavity during filling and solidification. The results of temperature distribution in the casting at different time steps during solidification are then coupled with the microscopic model to make porosity predictions. In our model, the macroscopic model is solved by a commercial software package.

Basic Equations

The microscopic model constitutes the mass balance equation for both metal and gas. Darcy's law is used to model the motion of interdendritic flow. Sievert's law is then used to calculate the local concentration of hydrogen:

1. Continuity Equation:

$$\frac{\partial \rho}{\partial t} + \nabla \cdot (\rho \bar{u}) = 0 \quad (1)$$

where ρ is density, t is time and u is the interdendritic flow velocity vector.

2. Motion Equation:

$$\bar{u} = -\frac{K}{\mu f_L} (\nabla P_s + \rho_L g) \quad (2)$$

where u is the interdendritic flow velocity vector, K is the permeability of the medium, μ is viscosity, f_L is volume fraction of liquid, P_s is shrinkage pressure, ρ_L is density of liquid and g is acceleration due to gravity. The permeability is defined as [12]

$$K = \frac{f_L^3 d_2^2}{180(1-f_L)^2} \quad (3)$$

where d_2 is the secondary dendrite arm spacing.

3. Hydrogen Mass Balance Equation:

$$[H_o] \rho_L = [H_s] \rho_s f_s + [H_L] \rho_L (1 - f_s - f_v) + \alpha \frac{f_v P_g}{T} \quad (4)$$

where H_o is the initial hydrogen content in the melt, H_s and H_L are the hydrogen content in the solid and liquid. ρ_L and ρ_s are the densities for liquid and solid metal, f_s and f_v are the volume fraction of solid and porosity. α is gas conversion factor, P_g is gas pressure, and T is the local temperature. The mass concentration of hydrogen dissolved in solid and liquid metal is given by Sievert's law:

$$[H_s] = K_s P_g^{1/2} \quad \text{and} \quad [H_L] = K_L P_g^{1/2} . \quad (5)$$

The condition for formation of a gas pore of radius r is:

$$P_g \geq P_o + \rho_L g h + P_s + P_\sigma \quad (6)$$

where P_g is the gas pressure, P_o , $\rho_L g h$, P_s and P_σ are the ambient pressure, metallostatic pressure, shrinkage pressure and surface tension between gas and liquid, respectively. P_o and $\rho_L g h$ are usually constants. P_g , P_s and P_σ need to be calculated in the model. Equation 6 shows that the gas pore can form only when its pressure is large enough to overcome the total local external pressure.

Probabilistic Model

The probabilistic model to simulate dendrite growth uses the mapping technique developed by others to predict grain structure [16,20]. A 2-D grid is generated for a given slice of the casting where porosity prediction is of interest. Each *element* is mapped to a much finer grid of *cells*. The cell size should be smaller than that of the secondary dendrite arm spacing because pores usually nucleate between secondary dendrite arms.

The randomness of our probabilistic model lies in the selection of solid cells, pore nucleation locations and pore growth direction within each element. Formation and growth

of pores are governed by the mathematical model described in previous section. Shrinkage pores, which are modeled by means of checking the surrounding cells of a liquid cell, is treated as a gas pore. Due to high diffusivity values, some hydrogen atoms that are dissolved in the metal will move to the shrinkage pores and recombine as hydrogen gas. Also, the fact that gas pores are usually nucleated near the dendrite tips are taken into account. The effect of grain refiners and grain modifiers on porosity formation is not considered at present stage, however, it will be included in future work.

Calculation Procedure

Cells at different state are represented by different numbers, e.g. 1 stands for solid, 2 for microshrinkage pore, 3 for gas pore and 4 for potential gas pore. In the post processor, different numbers will be converted to corresponding colors. Therefore, locations and sizes of pores can be visualized.

The flow chart for the model is shown in Figure 1a. The macro-model to simulate molten metal filling and solidification is first solved with casting process simulation programs. During the solidification process, the temperature and solid fraction distributions are calculated and recorded. These simulation results are coupled with the proposed micro-model to predict porosity evolution.

First time step of the program selects some nucleation sites in every element randomly. The number of nucleation sites depends on the value of solid fraction, f_s , at the beginning of solidification process. In the subsequent time steps, the solid cell growth is simulated according to an algorithm that liquid cells which are neighbors to solid cells have higher priorities to become solid cells. Though this is just a first order approximation model for cell growth simulation, it suits the purpose to study and verify our porosity prediction model.

After the selection of solid cells the program checks for the possibility of microshrinkage porosity formation (see flow chart). When a location was isolated by the neighboring dendrite structures, there is no path for the liquid metal to feed and compensate for the solidification shrinkage. Such location will eventually become a microshrinkage pore. Further study for the diffusive movement of hydrogen in the solid metal is needed in order to compute the amount of hydrogen trapped in the pore accurately. Presently, it is assumed that the amount of hydrogen trapped inside the microshrinkage pore is equal to that of gas pore with the same size.

EXPERIMENT

Figure 1b shows a schematics of the experimental setup. The plate-like castings were made by permanent mold gravity casting process. The molds were made of steel and had dimensions of 82mm x 275mm x 285mm. The plate-like castings were made of aluminum alloy A356. This alloy was chosen because it is one of the most widely used alloys in the industry. The castings had dimensions 7mm x 50mm x 150mm. Some sections of the castings were designed to have different thickness to investigate the effects of geometry on the formation of porosity.

Twelve thermocouples (type K) in six pins were installed along the vertical axis of mold cavity at a distance of 2 mm and 8 mm below pin surface. There were six air cooling pipes

on each side of the die. The melt was heated and kept at approximately 695C. The initial temperature of the mold was approximately 33C. Hydrogen content ranges from 0.02 to 0.29 ml/100g as determined by an AISCAN system. In cases where reduced hydrogen contents were required, melt was purged with Argon. When it was necessary to increase the hydrogen contents, fluxing the melt with chemical $\text{Na}_2\text{BO}_4\text{-H}_2\text{O}$ were introduced. The density in each specimen was measured by precision density measurement technique. The amount of porosity was then calculated. The locations of the specimen for density measurement are shown in Figure 2a.

RESULTS AND DISCUSSION

The macroscopic heat transfer problems is solved by the MAGMASoft commercial casting simulation software. Figure 2b. compares the calculated cooling curve for thermocouple 2 with experimental measurement. The comparison showed a good agreement. Casting made in cycle 10 was chosen as a sample casting for analysis and testing the proposed porosity prediction model. The initial hydrogen content for this sample casting was 0.203 ml/100g.

Specimen located on the center line, near the top of the casting (geometry was thicker) had highest amount of porosity (i.e. specimen E and G). On the contrary, specimen located on the sides, near the bottom of the casting had significantly less amount of porosity (i.e. specimen B, D). It was also observed that in general when the initial hydrogen content was increased, the amount the porosity in the casting was also increased.

After the macroscopic problem is solved, the results from one slice of the test piece casting were taken and coupled with the proposed 2-D program. For simplification, the following assumptions are made during calculation:

1. The dendrite structure of the casting is equiaxed.
2. Hydrogen that is dissolved in the melt can not escape through the mold. This is usually true for permanent mold castings.
3. Hydrogen is homogeneously distributed in the entire casting.
4. The hydrogen solubility limit did not change due to segregation during solidification.
5. Gas pore growth rate is relatively slow compared to the solidification process.
6. Gas pore does not move once it is formed.

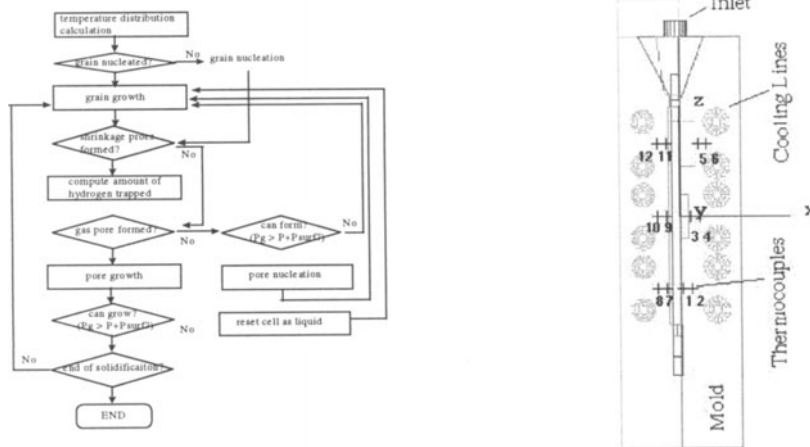


Figure 1a). Flow chart of the model. 1b). Schematic of the experimental setup.

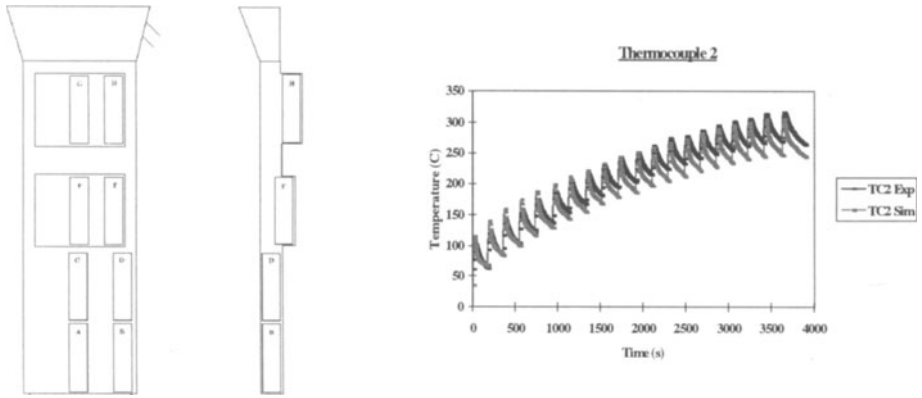


Figure 2a). Specimen locations. 2b) Comparison of calculated and experimental cooling curves.



Figure 3a. Comparison of calculated and experimental amount of porosity. (top: exp. bottom: calculated); 3b. Distribution of porosity from calculation.

Figure 3a. compares calculated and measured amount of porosity. The calculated result resembles the experimental one. In both cases, the specimen located on the centerline of the casting have higher amount of porosity than the ones on the side. Specimen located on top of the casting have higher amount of porosity than those at the bottom. However, the calculated result tends to underestimate the amount of porosity. The reason might be that the predicted results is from a 2D slice of the casting while the precision density measurement measures volumetric porosity. In some cases, especially for specimens located near top of the casting, macroshrinkage could form because of insufficient gross feeding. Since the proposed model only accounts for microporosity, it is expected that the predicted amount of porosity will tend to be lower. Figure 3b. shows the calculated distribution of porosity for the entire casting. The black dots represent the microporosity from prediction. It is shown that there are more pores on top of the casting and the pores are larger in size when compared to the bottom of the casting. This result agrees with the trend that is demonstrated in Figure 3a. Figure 4 shows the porosity predictions for each specimen with

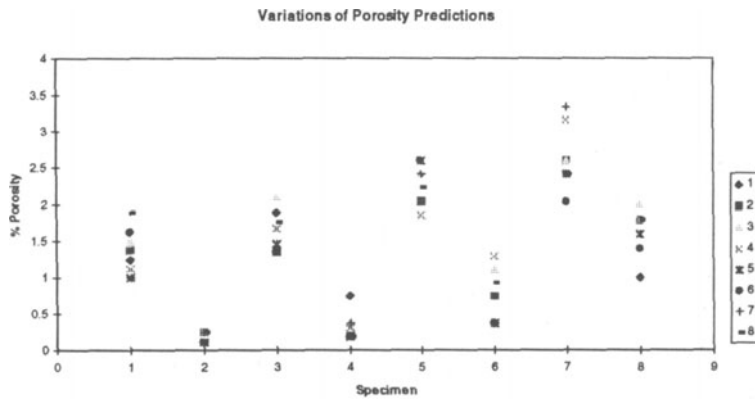


Figure 4. Variation of porosity predictions for specimens in eight simulation runs.

eight simulation runs. Due to the probabilistic nature in the model, the predicted amount of porosity varies with each run. However, as can be seen from the figure, the values are on the same order and the trends are fairly consistent.

CONCLUSIONS

A two dimensional model that integrates the mathematical model of porosity prediction with probabilistic model of grain nucleation and growth is examined. This model is able to predict microporosity not only in terms of the amount, but also the possible size and location. The preliminary examination of the model shows promising results, however, further work is needed to refine and validate the model.

ACKNOWLEDGEMENTS

This work has been supported by a NIST grant in cooperation with the Iowa State University Center for NDE and the Northwestern University Center for Quality Engineering and Failure Prevention. The authors would like to thank Jan Achenbach, Joe Gray, Morris Fine and Brian Moran for their assistance during the performance of this research.

REFERENCES

1. *Metals Handbook*, ASM International, vol. 15, 9th Edition, 1988.
2. J.A. Eady and D.M. Smith, "The Effect of Porosity on the Tensile Properties of Aluminum Alloy Castings", *Mat. Forum*, 9(4), 1986, pp217-223.
3. M.J. Couper, "Casting Defects and the Fatigue Behavior of an Aluminum Alloy Casting", *Fatigue Fracture Engineering Material Structure*, 13(3), 1990, pp213-227.
4. M.K. Surappa, "Effect of Macro-Porosity on the Strength and Ductility of Cast Al-7Si-0.3Mg Alloy", *Scripta Metallurgical*, 20, 1986, pp1281-1286.
5. D. Altenpohl, *Aluminum Viewed from Within*, Aluminum-Verlag, 1982.
6. M. Flemings, *Solidification Processing*, McGraw-Hill, 1974.
7. E. Niyama, T. Uchida, M. Morikawa and S. Saito, "A Method of Shrinkage Prediction and Its Application to Steel Casting Practice", *49th International Foundry Congress*, 1982.
8. K. Tynelius, J.F. Major, D. Apelian, "A Parametric Study of Microporosity in the A356 Casting Alloy System", *AFS Transactions*, 1993, pp401-413.

9. H. Huang, J.T. Berry, "Evaluation of Criteria Functions to Minimize Microporosity Formation in Long-Freezing Range Alloys", *AFS Transactions*, 1993, pp669-675.
10. N. Tsumagari, C.E. Mobley, P.R. Gangasani, "Construction and Application of Solidification Maps for A356 and D357 Aluminum Alloys", *AFS Transactions*, 1993, pp335-341.
11. J. Huang, *Study of Criteria Function for Porosity Prediction in A 356 Casting*, Master Thesis, Mechanical Engineering, Northwestern University, Dec. 1995.
12. K. Kubo, R. Phelke, "Mathematical Modeling of Porosity Formation in Solidification", *Met. Transactions B*, 16B, June 1985, pp359-366.
13. Q.T. Fang, D.A. Granger, "Porosity Formation in Modified and Unmodified A356 Alloy Castings", *AFS Transactions*, 97, 1989, pp989-1000.
14. S. Shivkumar, D. Apelian, J. Zou, "Modeling of Microstructure Evolution and Microporosity Formation in Cast Aluminum Alloys", *AFS Transactions*, 98, 1990, pp897-904.
15. J.D. Zhu and I. Ohnaka, "Computer Simulation of Interdendritic Porosity in Aluminum Alloy Ingots and Casting", *Modeling of Casting, Welding and Solidification Processes*, V, 1991, pp. 435-442.
16. J.L. Spittle and S.G.R. Brown, "Computer Simulation of the Effects of Alloy Variables on the Grain Structures of Castings", *Acta Metallurgica*, 37, 1989, pp1803-1810.
17. P. Zhu and R.W. Smith, "Dynamic Simulation of Crystal Growth by Monte Carlo Method-I. Model Description and Kinetic", *Acta Metallurgica*, 40, 1992, pp683-692.
18. M. Rappaz, Ch-A. Gandin, "Probabilistic Modelling of Microstructure Formation in Solidification Process", *Acta Metallurgica*, 41, 1993, pp345-360.
19. G.K. Upadhyaya, K.O. Yu, M.A. Layton, and A.J. Paul, "Probabilistic Modeling of Solidification Grain Structure in Investment Castings", *Modeling of Casting, Welding and Solidification Processes*, VII, 1995, pp. 517-523.
20. B. Szpunar and R.W. Smith, "Monte Carlo Simulation of Solidification Process; Porosity", *Canadian Metallurgical Quarterly*, 35, No.3, 1996, pp299-303.